Journal of Power Sources 191 (2009) 159–164

Contents lists available at ScienceDirect

Journal of Power Sources

journal homepage: www.elsevier.com/locate/jpowsour

Short communication

Negative plate macropore surfaces in lead-acid batteries: Porosity, Brunauer-Emmett-Teller area, and capacity

C.V. D'Alkaine*, G.A. de O. Brito

Group of Electrochemistry and Polymers, DQ-UFSCar, Rodovia Washington Luis, Km 235, CP 676, 13565-905 São Carlos (SP), Brazil

ARTICLE INFO

Article history:
Received 1 December 2008
Received in revised form 2 February 2009
Accepted 3 February 2009
Available online 11 February 2009

Keywords:
Single lead-acid battery plates
Macroporosity
Microporosity
Macropore surface roughness
Solid-state reaction
Negative plate

ABSTRACT

We propose an explanation for the production of an electrochemically active area during the electrochemical formation of lead-acid battery negative plates based on solid-state reactions. Our proposal is supported by experimental data. This study includes a critical review of the literature on charge/discharge mechanisms, porosity, and BET area. The critical review, through the latter two parameters, indicates the existence of both macro and micropores in positive plates, but only macropores in negative plates, with characteristic surface roughness. In the present paper the surface sulfation of the precursor is controlled using various acidic, neutral and alkaline solutions during an electrochemical formation process that does not include soaking. Our results confirm that variable roughness can be produced at the negative plate macropore surfaces. The morphological changes produced by different formation conditions are assessed by measuring the macroporosity, BET area, and capacity of single negative plates. Based on these concepts, a method was developed and applied to measure independently the contributions of geometrical surface macroporosity and roughness to the negative plate capacity.

1. Introduction: a critical review of the literature on reaction models and active material morphology

Thus far, fundamental research on chemical reactions in lead-acid battery systems has focused on charge/discharge processes. There are two main theories about the discharge of lead-acid battery negative and positive plates. The more generally accepted theory assumes that $PbSO_4$ formation occurs through a dissolution–precipitation mechanism [1]. This process consists of Pb^{2+} dissolution, super-saturation of the solution, nucleation of $PbSO_4$ crystals, and growth of the nuclei, all of which give rise to a discontinuous film. The other theory [2] assumes that though there may be some small initial dissolution process; the primary mechanisms are solid-state reactions, including nucleation, growth and subsequent collapse of the nuclei, growth of the resulting continuous film via a high electric field mechanism and, finally, the partial external disruption of this film followed by recrystallization of the disrupted part.

On the negative plate, the discharge process directly gives rise to two $PbSO_4$ films, one glued and one disrupted, as is discussed in a previous paper [3]. On the positive plate, this process first gives rise to a PbO film [2,4] that, when partially disrupted, would be converted into $PbSO_4$ through a chemical reaction with H_2SO_4, with the remaining PbO film remaining adhered to the PbO_2 surface [5]. The reduction of PbO_2 in positive plates has also been demonstrated to follow a zone reaction mechanism [4]. It must be pointed out that, in the case of positive plates, a model of a gel region inside the PbO_2 active material must be added to these two mechanisms at the point where the electrochemical reaction would take place [6]. If the gel model is taken to be on the surface of the PbO_2 [7], the gel reaction mechanism is in some ways equivalent to that of the solid-state reaction.

For charge processes, the literature is in general agreement that the dissolution–reduction (negative plates) and dissolution–oxidation (positive plates) mechanisms occur in a narrow gap between the discharge products and the active materials [1,8]. Nevertheless, it has been proved for flat negative electrodes [3] that some part of the discharge product always remains attached in a glued form to the electrode surface; thus, this glued film can be directly reduced by a solid-state mechanism in the context of a high electric field. This direct reduction [3] proves the presence of a glued $PbSO_4$ film in negative plates because the time required for this reduction should be much shorter than that required for a dissolution–precipitation mechanism. Due to the low solubility of $PbSO_4$, the remaining disrupted discharge product must remain in the form of a disrupted film, attached by surface forces to the glued film. The disrupted film will be reduced in a second step only through a dissolution–precipitation mechanism. This second process cannot be observed electrochemically. For the positive plate it has been voltammetrically shown that

* Corresponding author. Tel.: +55 16 3351 8077; fax: +55 16 3351 8350.
E-mail address: dalkaine@dq.ufscar.br (C.V. D'Alkaine).

0378-7753/$ – see front matter © 2009 Elsevier B.V. All rights reserved.
doi:10.1016/j.jpowsour.2009.02.002

part of the discharge product can be directly re-oxidized to PbO_2 [8] with much shorter relaxation times than those needed for a dissolution–precipitation mechanism even when the author has not realized this fact. This indicates that some part of the discharged film also remains glued to the PbO_2 active material and thus demonstrates the presence of a glued film in the positive plates as well. This film could be a Pb(II) oxide solid compound such as PbO. The direct formation of a $PbSO_4$ film is not assumed to occur via a solid-state reaction in the case of PbO_2 reduction in positive plates, because this would mean the SO_4^{2-} ion was moving against the reducing electric field through the film. Rather, the O^{2-} will be able to leave the PbO_2 surface assisted by the reducing electric field, leaving behind some form of PbO. The rest of the discharge product on the positive plates must also remain disrupted and attached by surface forces to the glued film; however, as the disrupted oxide film is no longer subject to high potentials, it should react with the H_2SO_4 to create a disrupted $PbSO_4$ film. It is well known that such disrupted films are present in positive discharged plates.

All these facts mean that two steps must take place during the charging. The first brings about the recovery of the glued films ($PbSO_4$ glued film in the negative plates and PbO glued film in the positive plates) through a solid-state reaction in the context of a high electric field [3,8]. The second step leads to the recovery of disrupted films via a dissolution–precipitation mechanism. This second step can occur through a narrow gap between the discharge-disrupted $PbSO_4$ (in either negative or positive plates) and the active materials [1,8] or directly through a normal dissolution–precipitation process that involves the disrupted particles [2]. An interesting point is that the dissolution–precipitation mechanism alone does not explain the voltammetric results [3,8], because it cannot explain the high rates at which part of the discharge products (the glued films) from the electrodes can be voltammetrically recovered as original products. Furthermore, the dissolution–precipitation mechanism alone does not explain why rotating the electrode has no effect on the whole film formation process, as has been experimentally demonstrated for the negative case [9].

Shifting our attention now from charge/discharge processes to the formation of active materials on the plates, some papers have a technological focus [10–12], while a others deal with reaction mechanisms and structures for negative [13,14], for positive [15–19] and for both plates [20]. This mechanistic issue is important because it is the production processes of active materials which give rise to their morphologies in both negative and positive plates. It is at the surfaces of these plates that the charge/discharge mechanisms discussed above would occur. With this in mind, the research presented herein proposes an explanation for the role of precursor/paste sulfation in negative plates with regard to the appearance of active electrochemical areas: the role of soaking process.

The large electrochemically active areas, as measured by BET, are considered the source of the high capacity for electrochemically produced active masses, both negative (NAM) and positive (PAM). It is well known that the electrochemically formed Pb and PbO_2 active materials exhibit much greater electrochemical activity than the sintered chemically produced ones [20]. The measured BET areas are larger for PAM than for NAM [21]. This can be attributed to the existence of macroporosity and microporosity in the electrochemically produced positive active materials, and to macroporosity alone in electrochemically produced negative active materials. This can be based on the following facts. On the positive plate, it is possible [21] to vary the BET area appreciably (from 4 to 11 $m^2\,g^{-1}$) without varying the macroporosity (which remains, for example, between 45% and 50%). This does not occur in the case of negative plates, where the BET area remains practically constant in the literature (about 0.5–0.8 $m^2\,g^{-1}$), while the macroporosity varies from 55% to 75% [21]. Furthermore, for negative plates, the area as calculated from the Hg porosimeter or other equivalent penetration measurement methods is equivalent to that obtained from BET adsorption measurements [21], whereas for positive plates the Hg porosimeter or equivalent penetration methods suggest areas about 10 times smaller than the results of BET experiments. This means that techniques such as the Hg porosimeter deliver the same measurements as BET on negative plates but different ones on positive plates. This difference suggests the hypothesis that microporosity exists on the macropore surfaces of positive plates, but that only roughness is found on the macropore surfaces of negative plates. This roughness will depend on the formation conditions, as will be demonstrated in the present paper. This roughness, as far as we know, have not been discussed in the literature. Nevertheless, in situ atomic force microscopy (AFM) seems to support this idea [22]. In all this context, the concepts of macro and microporosity, rather than in a previous definition of pore diameter, are based on kind and conditions of measurements like N_2 sorption, Hg penetration or liquid sorption methods, which give, in some cases, different results for negative and positive active materials.

Another matter not yet raised in the literature is that these BET area differences between negative and positive active materials should imply the need for very different amounts of active materials to be used in NAM and PAM during lead-acid battery construction; however, this is not seen in practice. This can only be explained if the negative films formed are thicker than the positive ones, in which case the two reaction products must be different and, in contrast to what the dissolution–precipitation mechanism proposes, cannot consist only of $PbSO_4$. This observation is also novel, to the best of the authors' knowledge.

The augmented BET area of PAM seems to be related to the acid concentration during the soaking and forming operations, and is not necessarily a factor of the soaking time, at least when the acid concentration and the soaking time are sufficient to produce maximum sulfation [23]. As far as we know, no explanations have been proposed as to how and why this increase in the BET area occurs.

It is commonly acknowledged that a high partial reduction in volume is associated with the change from $PbSO_4$ to Pb or PbO_2 [20]. Also, the precursor/paste is known to be sulfated at the pore surfaces during soaking and even during the first step of formation, due to the fact that the pore radii diminish [23]. The sulfation process has been shown for both the negative [13] and the positive [15] plates. Nevertheless, in the passage from the precursor to the active material, there is a high increase in BET area only on the positive plates [21]. A normal paste has a BET area of about 1–2 $m^2\,g^{-1}$ [21]. The BET area increase does not occur on the negative plates, and in fact there is some reduction in BET area here [21]. This is further evidence that micropores exist only in the positive plates.

Both macro and microporosity can be measured by the BET method [24], as shown in Fig. 7 of this reference. The Hg porosimeter [25] or the measurement of porosity through water [26] or glycerol [21] absorption only enables measurement of the macroporosity. However, these measurement techniques can present some problems in the case of negative plates, depending on the experimental conditions. The Hg porosimeter produces lead amalgams, and the water absorption (when oxygen is not totally removed) or glycerol absorption (when the glycerol is not completely free of adsorbed water) gives rise to lead corrosion.

The objective of the present article is to propose a solid-state reaction model explaining the variation in the BET areas and the electrochemical activity in electrochemically formed active materials, in the context of new experimental evidences. Data are presented for negative plates; experimental work is in progress on positive plates.

The central idea for negative plates is that, during the reduction of $PbSO_4$, the marked reduction in its volume can give rise to variable rugosity on the macropore surfaces of the Pb active material.

If all the other conditions remain constant, a decrease in the degree of precursor surface sulfation effected by eliminating soaking time and reducing the sulfation during electrochemical formation (by less acidic, neutral, or alkaline formation solutions) should reduce plate capacity (normally measured as, e.g. 4.6 M H_2SO_4). To test this, the precursor was formed in Na_2SO_4 solutions with various acid, neutral, or alkaline pHs, under the general assumption that the solution for precursor sulfation should be acidic. To determine experimentally whether the sulfation process is related to the real active area, parallel measurements were made of the water macroporosity and BET area, and these in turn were related to the electrochemical active area as measured through the capacity of the plates.

2. Experimental

The used non-formed negative plates (measured capacity, after normal forming, 10.65 ± 0.5 Ah plate^{-1} at a $C_{23.7\pm0.2}$ in 4.6 M H_2SO_4) were factory-produced, pasted with $3PbO{\cdot}PbSO_4{\cdot}H_2O$ plus PbO (without additives), and cured. The thickness of the non-formed plates was 2.0 mm, and the total surface area of the double face totalled 280 cm^2; to which all the current density measurements refer. The amount of precursor material in the plates was 85 ± 2 g plate^{-1}, and its macroporosity (before formation) was 42 ± 2%. Macroporosity was always measured using the water absorption method. The final amount of Pb after formation was 75 ± 3 g plate^{-1}.

The experimental system was a cell in which two positive charged plates were rigidly located, as counter-electrodes, at a distance of 4 cm from both sides from the central working negative plate, with the same geometrical areas. This was done so as to work at constant external solution concentrations. The Hg/Hg_2SO_4/4.6 M H_2SO_4 reference electrode, against which all potentials are given, was located just in front of one of the faces of the central working negative plate.

The formation solutions were 1.0 M Na_2SO_4, used as supporting electrolyte and supplier of SO_4^{2-} anions, plus a given low concentration of NaOH or H_2SO_4 to fix the formal pHs. The various chosen formal pHs will be discussed in Section 3. In some cases a normal 1.0 M H_2SO_4 formation solution, without Na_2SO_4, was used for comparison (formal pH 0.0). In all cases, the discharge solutions were 4.6 M H_2SO_4. A new plate was used in each experiment, after having been previously formed in one of the above solutions. The forming current density (i_f) was always 5 mA cm^{-2} (or 18.7 mA g^{-1} of lead), and the formation time (t_f) was equal to or longer than 100 h to assure complete formation. After each formation, the solution was changed to 4.6 M H_2SO_4, even inside the pores of the plate. The plates were then partially cycled in order to complete the formation process; about five cycles were needed for this, with a discharge current density, i_d, of 1.6 mA cm^{-2} (6.0 mA g^{-1} of lead) for 4 h, followed by a charge current density, i_{ch}, of 0.4 mA cm^{-2} (1.5 mA g^{-1} of lead) for 20 h.

To determine the average capacities ($\langle C \rangle$), several discharges were made up to a cutting potential of −0.7 V, in 4.6 M H_2SO_4 solution. These capacities were determined with a constant i_d of 1.6 mA cm^{-2} (6.0 mA g^{-1} of lead), a C_{24} capacity for the negative plate formed in 1.0 M H_2SO_4. This i_d was chosen to minimize concentration gradient limitations at the cutting potential. Between each capacity determination, the plates were recharged in the same solution with an i_{ch} of 0.4 mA cm^{-2} (1.5 mA g^{-1} of lead), passing a charge equivalent to at least 1.4 times the previously obtained capacity to ensure recharge.

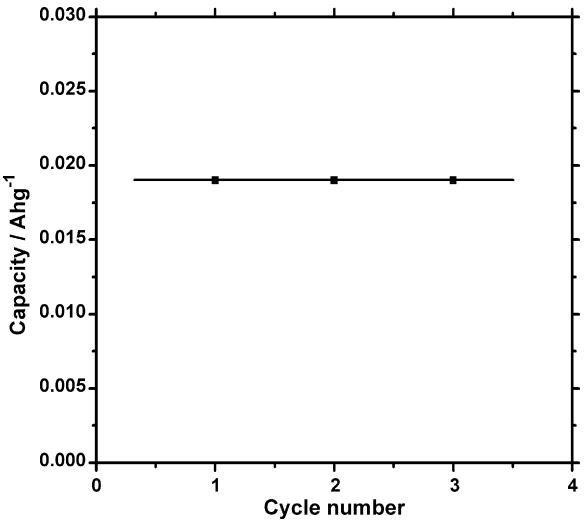

Fig. 1. Capacity of a negative plate in successive discharges in 4.6 M H_2SO_4. Plate formation solution: 1.0 M Na_2SO_4 plus 0.1 M NaOH.

The reproducibility of the capacity measurements for one case (formation in 1.0 M Na_2SO_4 plus 0.1 M NaOH) is given as an example in Fig. 1, where the low capacity value is related to being formed in an alkaline pH, as will be seen in the next section.

Since dissolution of the precursor can occur during formation in alkaline solutions, experiments immersing the precursor in 0.1 M NaOH (the most alkaline solution used) together with 1.0 M Na_2SO_4 were carried out over 150 h (1.5 times the formation time used), to test the importance of dissolution. The results show a loss in precursor weight of no higher than 3.5% (by weight) after 150 h, indicating that the dissolution of precursor during formation can be disregarded, even for solutions with high pH. This result might have been expected because the presence of Na_2SO_4, through the common ion phenomenon, should inhibit the dissolution process.

3. Results and discussion

Our aim was to study the influence of precursor sulfation on the morphology of the resulting spongy Pb when the soaking step is eliminated and the formation solution pH is controlled in order to regulate sulfation.

It should be noted that the formation of negative plates is accompanied by a rise in the pH of precursor pore solutions due to the reduction of PbO and $PbSO_4$ to Pb. These reductions will lead to the consumption of H_3O^+, converting O^{2-} ions of PbO to H_2O and SO_4^{2-} ions of $PbSO_4$ mainly to HSO_4^-. Hence, it is possible for the formation solution to exhibit alkaline pHs. The solution pH was changed by adding NaOH or H_2SO_4 to the 1.0 M $NaSO_4$ formation solutions, and the pH was in this way practically controlled in the precursor macropores during formation. The 1.0 M Na_2SO_4 solutions were used as supporting electrolytes and to donate SO_4^{2-} and HSO_4^- ions, depending on solution pH.

The formation process in negative plates, elucidated from the ideas of Takehara [1,8], can be described as the result of a dissolution–reduction reaction occurring in a narrow gap between the already formed spongy Pb and the still unreacted precursor. It is this kind of metasomatic process that makes the original morphological characteristics of the precursor so important. Fundamentally, it seems that the reduction of the precursor first occurs in bulk, followed by the reduction of the $PbSO_4$ formed by sulfation at the pore surface.

In this context, the first part of the study investigated the effects of the formation conditions (various formation solution pHs) on macroporosity. These results can be seen in Fig. 2.

The macroporosity of negative active mass is fundamentally determined by the precursor macroporosity at the time of pasting, due to the metasomatic formation process. The precursor macroporosity is determined by the amount of free residual water remaining in the precursor/paste [27]. As a consequence, since all pastes used in this study have the same water content, the macroporosity of NAM in the various formation solutions should not be expected to change with solution pH. Fig. 2 confirms that the pH of the formation solution does not affect the negative plate's macroporosity. The significance of this observation is that any change in BET area or plate capacity should not be attributed to variation in the NAM macroporosity.

The average porosity of NAM spongy Pb was $62.5 \pm 2.5\%$ (Fig. 2), representing an increase in porosity of about 50% through the transformation from precursor to spongy Pb. This increase in the macroporosity from the precursor to spongy Pb, even involving a metasomatic reaction, is assumed to be due to the reduction in volume as the precursor (whether $PbSO_4$ or $3PbO{\cdot}PbSO_4{\cdot}H_2O$, due to their high partial volumes when compared with Pb) is converted to the spongy Pb.

The second part of the analysis investigated the influence of formation solution pH on the BET area of the formed plate. Our proposed hypothesis is that the variation of pH in the formation solution should be translated into a variation in NAM BET areas. The sulfation process would be responsible for varying the BET areas by varying the roughness of the macroporous inner surface of the NAM as it seems to be shown by AFM [22]. In the case of negative plates, as stated in the introduction, there are no experimental facts suggesting the existence of microporosity. For this reason the BET area of negative plates varies by a smaller amount than that of the positive plates, as demonstrated by our data, even at constant macroporosity. We propose that the variation in macropore inner surface roughness in negative plates is produced by the transformation of the sulfated $PbSO_4$, formed on the inner surface of macropores of the precursor during soaking and formation, to a Pb inner surface. This is due to the significant reduction in volume [20] that accompanies this process along with the specific solid-state reaction characteristics, since a solid-state transformation reaction involving a major reduction in volume will not necessarily give rise to a rough surface.

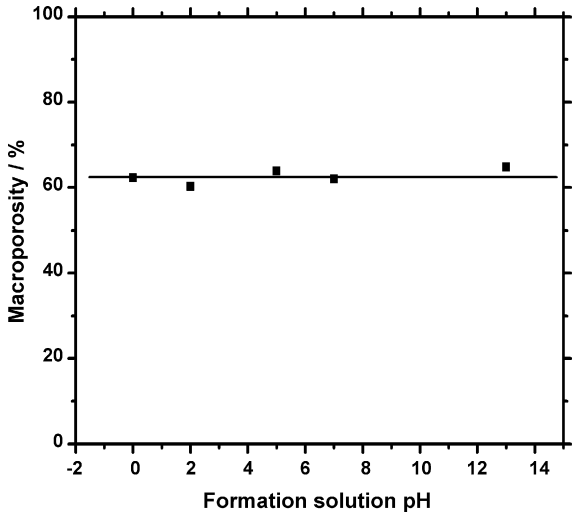

Fig. 2. Water absorption macroporosity of negative plate active material formed at various pHs. All other conditions were held constant. Each experimental point represents one plate.

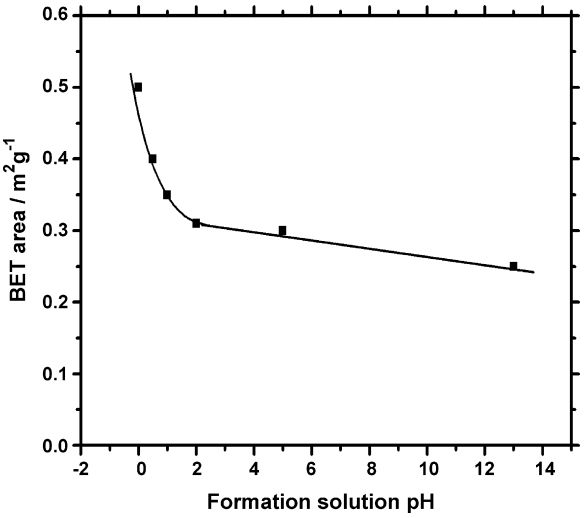

Fig. 3. BET area of negative plate active material formed at various pHs. All other conditions were held constant. Each experimental point represents one plate.

The results for the NAM BET areas obtained at various formation solution pHs can be seen in Fig. 3, where a formation in 1.0 M H_2SO_4 solution without Na_2SO_4 (formal pH 0.0) was also plotted to show the continuation of the curve up to normal formation conditions (formation pH about zero), and where the BET area yields the expected value for negative plates ($0.5\ m^2\ g^{-1}$).

In Fig. 3 a sharp fall is seen in the BET area between the formal pHs 0.0 and 2.0, where there is a significant decrease in H_3O^+ ion concentration. The presence of this ion at the precursor/solution interface seems to be a necessary condition for sulfation, possibly enabling a favorable inner potential difference at this interface. It is generally known that a precursor requires a sufficiently acidic solution in order to be sulfated. This can easily be proven by visually following the reaction between particles of the precursor and sulfate solutions with different pHs, because the formation of $PbSO_4$ on the surface of precursor particles turns them white.

On the other hand, for pHs between 2.0 and 13, Fig. 3 shows a small decrease in BET area of the spongy Pb on negative plates. From the point of view of the proposed model, this means that the sulfation process is practically constant over this pH region, though it seems to occur more slowly as pH rises.

A third question to be analyzed was the influence of formation solution pH on the average capacities of the plate, $\langle C \rangle$. These results are shown in Fig. 4 and clearly indicate that reduction in sulfation at the inner pore surfaces of the precursor causes a reduction in the average capacity. For the purposes of the model, this shows that the roughness at the macropore inner surfaces of the NAM decreases with increasing formation pH, which is in accordance with the BET area measurements. Nevertheless, these two decreases (the BET area and the average capacity) do not happen in the same pH interval. The decrease of the average capacity occurred primarily between formal pHs 0.0 and 5.0–6.0 (Fig. 4), while the BET area decrease fell between pHs 0.0 and 2.0 (Fig. 3). This is a first indication that the BET area and the electrochemically active area do not have exactly the same physical meaning. One possible explanation is that between the BET area and the average capacity, the discharge film thicknesses must be influential. It is quite possible that the film thickness depends on the state of surface roughness; to research this question, a new plot was drawn in which average capacities were plotted against BET areas. These data can be seen in Fig. 5.

Before analyzing Fig. 5, it is important to note that for pHs higher than 5.0–6.0, the measured average capacity does not effectively change with formation pH. In terms of the proposed model,

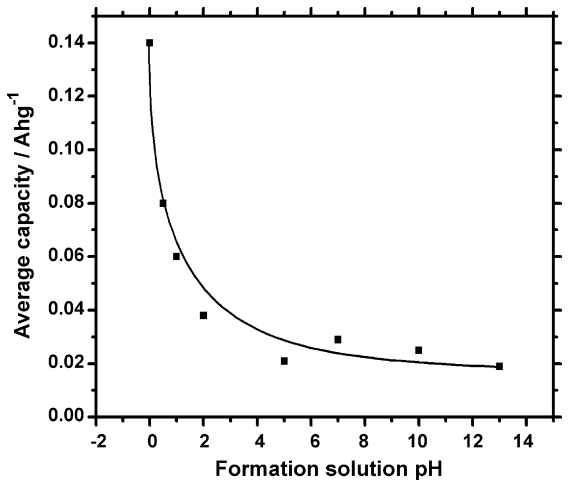

Fig. 4. Average capacities for negative plates formed at various pHs. All other conditions were held constant. Each experimental point represents one plate.

this means that there is practically no roughness variation at the macropore inner surfaces and thus no change in the discharge film thickness with formation pH over this range.

Fig. 5 can be interpreted as revealing two contributions to the average capacity, which are highlighted in the figure by two arrows. One of the contributions would correspond to the geometrical macropore area with practically no roughness ($\langle C\rangle_{gmc}$, geometrical macropore contribution). This is constant, like the macroporosity of the studied plates. The second contribution, beginning at a total BET area of 0.25 $m^2\,g^{-1}$, would correspond to the appearance of what we term the "macropore roughness contribution" ($\langle C\rangle_{mrc}$). This average capacity contribution changes with formation pH, consistent with the proposed model, and can include not only an increase in real area but also, perhaps, an increase in the free energy of the constant real area. As a consequence of this analysis, the thickness of the growing film could also increase.

Fig. 5 can therefore be interpreted as showing that the macropore geometrical surface contributes to the capacity at a constant value of 0.017 Ah g^{-1}. On the other hand, the capacity could reach up to 0.125 Ah g^{-1} due to the macropore roughness contribution, which in the present case changes almost linearly with BET area (see Fig. 5).

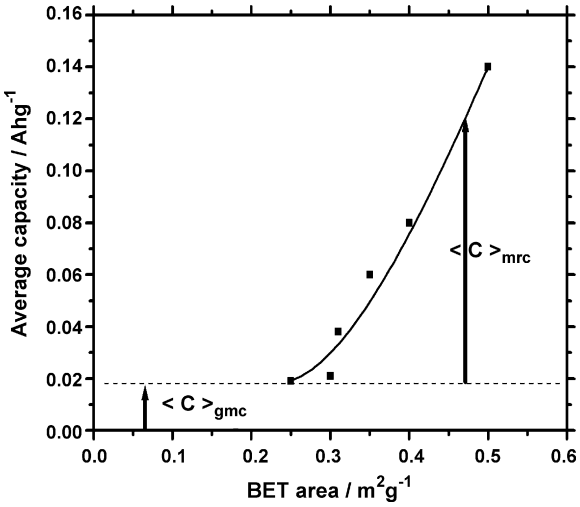

Fig. 5. Average capacities from Fig. 4 versus BET areas from Fig. 3, at the corresponding formation solution pHs. $\langle C\rangle_{gmc}$ geometrical macropore capacity contribution; $\langle C\rangle_{mrc}$, macropore roughness capacity contribution.

From plots such as those in Fig. 5, the contribution to the plate capacity of the macropore geometrical inner surfaces and the macropore surface roughness can be experimentally determined.

4. Conclusions

Based on a critical view of the literature, distinct morphological and solid-state reaction models are proposed for discharge and charge mechanisms in the context of both negative and positive single plates.

For negative plate morphology, the proposal includes macroporosity inside the active material and varying roughness levels on the macropore inner surfaces. We propose that the discharge mechanism is consistent with a minor initial dissolution process followed by $PbSO_4$ solid-state nucleation, growth and collapse of the nuclei to form a continuous film, growth of the continuous film through a high electric field mechanism, and finally, partial external disruption of this $PbSO_4$ film followed by recrystallization of the disrupted part. A glued $PbSO_4$ film then remains at the spongy Pb active material surface. The charging process is hypothesized to include a first step wherein the remaining glued $PbSO_4$ film is reduced to Pb by a high electric field mechanism, and after which the disrupted $PbSO_4$ film can be reduced by a dissolution–precipitation mechanism. The latter process may follow the typical description (dissolution of $PbSO_4$ crystals followed by a precipitation–reduction mechanism) or may occur in a narrow gap between the disrupted $PbSO_4$ crystals and the already recovered spongy Pb. The narrow gap advances in a metasomatic way during the charging process, eliminating the disrupted film.

For the positive plate morphology, also based on a critical view of the literature, the existence of both macro and micropores is proposed. The whole charge/discharge process is reported to be a zone reaction mechanism; it is at the macro and micropore surfaces that the charge/discharge reactions take place. During the discharge a minor initial dissolution process could also occur, but it is rapidly followed by a solid-state nucleation involving a solid oxide form of Pb(II), possibly PbO. The PbO nuclei grow and collapse, giving rise to a continuous film that grows via a high electric field mechanism. Finally, this PbO film is partially disrupted externally, generating a $PbSO_4$ disrupted film through reaction with H_2SO_4. The remaining PbO film is glued on the PbO_2 surface. Throughout the charging process, firstly, this remaining glued PbO film is oxidized through a high electric field mechanism. Thereafter, the disrupted $PbSO_4$ recrystallized film is oxidized either through a normal dissolution–oxidative process or by one confined within a narrow gap advancing from the PbO_2 surface into the $PbSO_4$ disrupted particles.

On the basis of these ideas, data are presented showing the production of variable BET area in negative plates, and a model for its physical interpretation is proposed and discussed.

As a result of measuring the characteristics of plates formed at different pHs (macroporosity, BET area and capacity), it has been shown that electroactive areas obtained in normal negative plate battery production are dependent on the level of precursor sulfation. We propose that it is the high partial volume reduction, when going from $PbSO_4$ sulfated precursor surface to the spongy Pb surface, that causes the variation in electrochemically active area; further, that this occurs through a variation in the precursor sulfation level controlling the roughness. This roughness variation can also induce an increase in film thickness during the discharge.

Finally, on the basis of these ideas, a method is developed and applied for measuring geometrical macroporosity and roughness capacities as separate contributions to the whole capacity.

Acknowledgments

Both authors are grateful to RONDOPAR Energia Acumulada Ltda for their support of the program to which the present work belongs.

References

[1] Z. Takehara, J. Power Sources 158 (2006) 825–830.
[2] C.V. D'Alkaine, L.M.M. de Souza, P.R. Impinnisi, J. de Andrade, J. Power Sources 158 (2006) 997–1003.
[3] C.V. D'Alkaine, C.M. Garcia, P.M.M. Pratta, G.A.O. Brito, F.P. Fernandes, J. Solid State Electrochem. 11 (2007) 1575–1583.
[4] C.V. D'Alkaine, A. Carubelli, M.C. Lopes, J. Power Sources 64 (1997) 111–115.
[5] C.V. D'Alkaine, P. Mengarda, P.R. Impinnisi, J. Power Sources, accepted for publication.
[6] D. Pavlov, G. Petkova, M. Dimitrov, M. Shiomi, M. Tsubota, J. Power Sources 87 (2000) 39–56.
[7] D. Pavlov, G. Petkova, J. Electrochem. Soc. 149 (5) (2002) A654–A661.
[8] Z. Takehara, J. Power Sources 85 (2000) 29–37.
[9] F.E. Varela, M.E. Vela, J.R. Vilche, A.J. Arvia, Electrochim. Acta 38 (11) (1993) 1513–1520.
[10] L.T. Lam, I.G. Mawston, D. Pavlov, D.A.J. Rand, J. Power Sources 48 (1994) 257–268.
[11] F. Steffens, J. Power Sources 31 (1990) 233–241.
[12] L. Prout, J. Power Sources 41 (1993) 195–219.
[13] D. Pavlov, V. Iliev, G. Papazov, E. Bashtavelova, J. Electrochem. Soc. 121 (1974) 854–860.
[14] D. Pavlov, V. Iliev, J. Power Sources 7 (1981/82) 153–164.
[15] D. Pavlov, G. Papazov, V. Iliev, J. Electrochem. Soc. 119 (1972) 8–19.
[16] D. Pavlov, G. Papazov, J. Electrochem. Soc. 127 (1980) 2104–2112.
[17] D. Pavlov, E. Bashtavelova, J. Power Sources 31 (1990) 243–254.
[18] L.T. Lam, H. Ozgun, L.M.D. Cranswick, D.A.J. Rand, J. Power Sources 42 (1993) 55–70.
[19] S. Grugeon-Dewaele, J.B. Leriche, J.M. Tarascon, A. Delahaye-Vidal, L. Torcheux, J.P. Vaurijoux, F. Henn, A. De Guibert, J. Power Sources 64 (1997) 71–80.
[20] D. Pavlov, in: D.A.J. Rand, P.T. Moseley, J. Garche, C.D. Parker (Eds.), Valve-Regulated Lead Acid Batteries, Elsevier, Amsterdam, 2004, pp. 37–108.
[21] E.E. Ferg, P. Loyson, N. Rust, J. Power Sources 141 (2005) 316–325.
[22] N. Hirai, D. Tabayashi, M. Shiota, T. Tanaka, J. Power Sources 133 (2004) 32–38.
[23] M. Dimitrov, D. Pavlov, T. Rogachev, M. Matrakova, L. Bogdanova, J. Power Sources 140 (2005) 168–180.
[24] L.T. Lam, O. Lim, H. Ozgun, D.A.J. Rand, J. Power Sources 48 (1994) 83–111.
[25] G.L. Corino, R.J. Hill, A.M. Jessel, D.AD.J. Rand, J.A. Wunderlich, J. Power Sources 16 (1985) 141–168.
[26] M.A. Wilson, M.A. Carter, W.D. Hoff, Materials and Structures/Matériaux et Constructions 32 (1999) 571–578.
[27] D. Pavlov, M. Dimitrov, T. Rogachev, L. Bogdanova, J. Power Sources 114 (2003) 137–159.